Proceedings of the 21st ICSMGE, Vienna, Austria, 14 – 19 June 2026. Pistrol, Adam & Schweiger (eds.)
Published by: ÖGG, Austrian Society for Geomechanics, Salzburg, Austria, ISBN 978-3-9503898-4-5
https://doi.org/10.53243/ICSMGE2026-1729

Impact of the concentration of sodium hydroxide NaOH on the compaction properties and strength of an alkali-activated-GGBS stabilized clayey silt

Diana Chami, Alessia Cuccurullo, Pierre Gerard
Université libre de Bruxelles (ULB), BATir department, Belgium, diana.chami@ulb.be

ABSTRACT: Alkaline activators are a key factor in alkali-activated systems, as they influence both chemical reactivity (by promoting the dissolution of the precursor) and physical performance (through their effect on compaction properties due to increased viscosity). This study investigates the effects of alkali activation using sodium hydroxide (NaOH) on the compaction behavior, pore size distribution and unconfined compressive strength (UCS) of a clayey silt stabilized with 5% alkali-activated ground granulated blast furnace slag (GGBS). Proctor compaction tests, mercury intrusion porosimetry tests (MIP) and UCS measurements were conducted on mixtures prepared with NaOH solutions of varying concentrations (2M, 4M, and 12M), in addition to non-activated GGBS for comparison. The results showed that the 2M NaOH mixture exhibited a slight increase in the maximum dry density (MDD) and a shift of the optimum moisture content (OMC) toward lower values, while higher concentrations (4M and 12M) led to reduced compactability and increased water demand. However, variations in activator concentration did not significantly affect the initial pore size distribution of the compacted soil (day 0), as all samples exhibited a similar bimodal distribution with consistent pore sizes. To isolate the effect of chemical reactivity from compaction, all mixtures were compacted to the same dry density and moisture content for UCS testing. The results revealed that the 2M mixture achieved the highest strength at all curing times (0, 7, 28 and 60 days), with strength decreasing at higher concentrations. The trends observed could be explained by the variations in the availability of free water influenced by ion hydration. The findings highlight the importance of balancing chemical activation with moisture availability to optimize the mechanical performance of alkali-activated soil systems.

KEYWORDS: Soil stabilization, alkali-activated materials, unconfined compressive strength, proctor compaction curve.

1 INTRODUCTION

Soil stabilization using alkali-activated materials (AAM) is gaining prominence as a more sustainable alternative to traditional methods such as lime or cement stabilization, by converting industrial aluminosilicate-rich waste into valuable binders. AAM emerged in the 1970s as a binding material to substitute ordinary Portland cement (OPC) (Davidovits 2002). A recent study demonstrated that producing 1 cubic meter of alkali-activated concrete with a compressive strength of 40 MPa requires 50% less energy and emits only one-third of the CO_2 compared to producing the same volume of OPC concrete with the same compressive strength (Alsalman et. al 2021). AAM are synthesized through the chemical activation of precursors such as fly ash (FA) or ground granulated blast furnace slag (GGBS), typically rich in silica (SiO_2) and alumina (Al_2O_3). An alkaline activator, commonly sodium hydroxide (NaOH) or potassium hydroxide (KOH), is used to initiate the dissolution of the precursor. Due to the high pH environment created by the alkaline activator, the Si-O-Si, Al-O-Al and Si-O-Al covalent bonds within the precursor material are broken down. This process releases Si and Al ions and hydration products start to accumulate and precipitate, leading to the formation of an aluminosilicate hydrate gel (N-A-S-H or K-A-S-H, depending on the type of activator used) (Myers et. al 2013). Additionally, if calcium is present in the precursor, a nanocrystalline product, known as calcium aluminosilicate hydrate C-A-S-H, is formed (Myers et. al 2013). While AAMs have been extensively studied in the context of concrete as substitutes for OPC (Alahmari et al., 2023), their application in soil stabilization is relatively more recent. Recent studies have shown that alkali-activated binders can significantly enhance the mechanical and durability properties of weak soils (Sahoo and Prasad Singh 2022, Al-Rkaby 2019, Ghadir and Ranjbar 2018, Coudert et al. 2021, Chami et al. 2024).

The performance of an alkali-activated stabilized soil depends on several factors such as i) the activator type and concentration; ii) the precursor type and mineralogy; iii) the soil type and grain size distribution and iv) the curing conditions to which the material is subjected (Myers et. al 2013). Among these, the activator is a key component in the production of AAM, but its use remains controversial. It can potentially contradict the main objective of this alternative binder, which is sustainability and a lower carbon footprint because producing 1 ton of NaOH generates nearly 999 kg of CO_2 (Ghadir and Ranjbar 2018). Therefore, it is crucial to use the activator efficiently to achieve optimal strength without excessive use.

In fact, in systems activated with NaOH, increasing the concentration leads to a higher availability of Na^+ and OH^- ions, which enhances the dissolution of reactive aluminosilicate phases present in the precursor (GGBS, a calcium rich precursor). This facilitates greater precipitation of binding gels, such as C–A–S–H, contributing to improved strength development. However, the increase in activator concentration also modifies the water dynamics within the system. As the ionic strength rises, a significant portion of the mixing water becomes bounded in hydration shells around the dissolved ions (Na^+ and OH^-), reducing the availability of free water (Onuki et. al 2011). This results in a more viscous and apparently drier mixture, adversely affecting compaction efficiency (i.e. lower dry density for a same energy of compaction). Furthermore, limited free water can inhibit the dissolution process by restricting the transport of the dissolved ions, thereby reducing the extent of gel formation. Consequently, while higher activator concentrations may enhance chemical reactivity, they can also lead to reduced densification and lower mechanical performance due to poor workability and restricted ion mobility. These competing effects underline the need to optimize both the moisture content and the activator concentration to achieve a balance between reactivity, workability, and compaction, thereby maximizing the mechanical performance of the stabilized soil.

Previous studies offer mixed conclusions regarding the optimal NaOH concentration. Ghadir and Ranjbar (2018) reported that increasing the concentration of the NaOH solution from 4 to 12 M while keeping the same activator content resulted in approximately a 50% increase in the unconfined compressive strength (UCS) of the clayey soil stabilized with

alkali-activated volcanic ash. In contrast, Cristelo et al. (2012) showed that for a silty sand stabilized with an alkali-activated low calcium FA, an optimal concentration of the activator exists and is a function of the mass ratio of the precursor to the activator. The differences in conclusions found in the literature can be attributed to variations in the precursor properties, curing conditions, and soil types. Hence, further research on these control parameters is necessary. Moreover, while some work has focused on strength development, fewer studies have examined how alkali activation influences the compaction behavior of the soil and, in turn, how compaction conditions affect the resulting strength, particularly with respect to the critical role played by the availability of free water .

So ultimately, this study aims to find that optimal balance, where we can achieve both sufficient chemical reactivity and efficient compaction in order to reach an optimal strength. For this reason, standard proctor compaction tests, mercury intrusion porosimetry tests (MIP) and UCS tests were performed on alkali-activated stabilized soil mixtures composed of a clayey silty soil with 5% GGBS and 2M, 4M and 12M NaOH solutions. In this context, MIP tests are useful for gaining a better understanding of how activator concentration influences the as-compacted soil microstructure, and of its subsequent effects on the strength of the stabilized soil.

2 MATERIALS AND METHODS

2.1 Materials

A clayey silt soil (referred to as MLD), classified as CL-ML under the Unified Soil Classification System (ASTM D2487-00), issued from the Marche-les-Dames region in Belgium, was used for this study. The soil was oven-dried for 24 hours prior to usage to eliminate moisture and ensure uniform conditions. As shown in Figure 1, the grain size distribution of MLD indicates a well-graded profile, with 79% of particles passing through the 75 µm sieve. The soil composition consists of approximately 13% clay, 62% silt, and 25% sand (Gerard et. al 2015). Based on ASTM D4318 standards, the liquid limit (LL), plastic limit (PL), and plasticity index (PI) were determined to be 28.4%, 19.6%, and 8.8%, respectively. Furthermore, the Standard Proctor test, carried out in accordance with ASTM D698, yielded an optimum moisture content (OMC) of 15.5% and a maximum dry density (MDD) of 1.82 g/cm³, as shown in Figure 2. The UCS of the MLD soil, compacted at the corresponding OMC and MDD and loaded at a displacement rate of 0.0667 mm/min, was approximately 145 kPa.

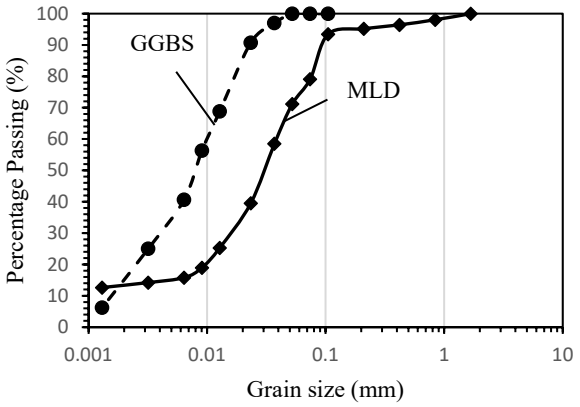

Figure 1: Grain size distribution of MLD soil and GGBS

Ground granulated blast furnace slag (GGBS), obtained from VVM Cement Company in Belgium, was used as the precursor material. As illustrated in Figure 1, its grain size distribution shows that 100% of the particles pass through the 75 µm sieve. GGBS was stored in tightly closed containers to avoid any moisture exposure. The X-ray fluorescence (XRF) analysis, shown in Table 1, shows that the main elements of GGBS are Ca, Si and Al, which together make up to 90% of its total mass.

Table 1. Chemical composition of GGBS and MLD.

Chemical composition	**Percentage by mass (%)**	
	GGBS	MLD
Calcium oxide (CaO)	43.15	0.69
Silicon oxide (SiO_2)	36.27	71.43
Aluminium oxide (Al_2O_3)	10.47	13.89
Magnesium oxide (MgO)	5.98	1.17
Sulphur oxide (SO_3)	1.51	0.02
Potassium oxide (K_2O)	0.67	2.52
Ferric oxide (Fe_2O_3)	0.58	4.27
Titanium oxide (TiO_2)	0.54	0.87
Manganese oxide (Mn_2O_3)	0.29	0.05
Sodium oxide (Na_2O)	0.26	0.77

As for the activator, a sodium hydroxide (NaOH) solution was used. The NaOH solution was prepared in the laboratory by dissolving NaOH pellets with 99% purity in distilled water to achieve the required concentration. It was prepared 24 hours prior to use to allow the heat generated during dissolution to dissipate.

2.2 Mix proportions and samples preparation

For the preparation of the alkali-activated GGBS-stabilized soil, a constant GGBS content of 5% by dry mass of MLD was chosen for all samples, based on preliminary results. The activator (NaOH) was applied at three different molar concentrations: 2M, 4M and 12M. For reference, a set of GGBS-stabilized samples without any activator was also prepared and tested.

MLD and GGBS were first mixed in dry conditions for 1.5 minutes at low speed using a MATEST mortar mixer to ensure uniformity. Subsequently, either a NaOH solution of the desired concentration (for alkali-activated GGBS-stabilized soil) or distilled water (for GGBS-stabilized soil) was added, and mixing was continued at high speed for an additional 2 minutes. The sample IDs and proportions are presented in Table 2.

Table 2. Sample IDs and composition.

Sample ID	**GGBS percentage (%)**	**NaOH concentration (M)**
MLD-H2O	-	-
MLD-5-H2O	5	-
MLD-5-2M	5	2
MLD-5-4M	5	4
MLD-5-12M	5	12

To isolate the effect of the compaction on the resistance of the stabilized soil, all the stabilized samples for the UCS and MIP tests were compacted at the OMC and MDD of the reference mix (MLD blended with 5% GGBS and water, named "MLD-5-H2O" in this study), as determined from the compaction curve shown in Figure 2, based on the standard Proctor test. The amount of NaOH solution (for alkali-activated GGBS stabilized soil) or distilled water (for GGBS stabilized soil), was set at 16.5% by mass of the solids mixture (MLD + GGBS), corresponding to its OMC, as determined from the standard proctor test conducted with distilled water. Moreover, cylindrical samples (72 mm in height and 36 mm in diameter) were dynamically compacted in three equal layers to achieve the MDD of the solids mixture, which was 1.79 g/cm3. To ensure interlayer bonding, the surface between each layer was

scrubbed before adding the next layer. After manual extrusion from the molds, the compacted samples were wrapped in plastic and aluminum foil to minimize moisture loss. The samples corresponding to a curing time of 0 days were directly tested after compaction and extrusion. The other samples were cured sealed for 7, 28 and 60 days in a controlled room temperature of ± 18 ℃ and a relative humidity of 50% until the day of testing.

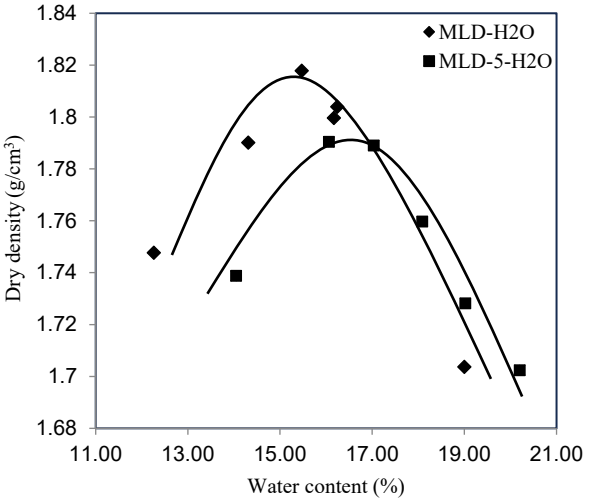

Figure 2: Grain size distribution of MLD soil and GGBS

2.3 Testing procedure

2.3.1 Compaction test

Standard proctor tests, in accordance with the ASTM D698 guidelines, were conducted on the MLD and GGBS mixture with NaOH solutions of different concentrations: 2, 4 and 12M. The samples were compacted in three layers in a 948 cm^3 mold, and 25 blows were applied for each layer using a 2.5 kg rammer, resulting in a compaction effort of 600 kJ/m^3. Scrubbing of the surface between each layer was performed to enhance interlayer bonding. The samples were compacted immediately after mixing to prevent particle aggregation and ensure uniformity, avoiding any premature reactions initiated by the alkali activation of GGBS.

2.3.2 Pore size distribution

To investigate the pore structure of the MLD and GGBS mixtures with various concentrations of NaOH, MIP tests were conducted using a Micromeritics Autopore IV apparatus with a maximum intrusion pressure of 414 MPa. The soil samples were compacted into cylindrical specimens measuring 72 mm in height and 36 mm in diameter, then broken into small pieces of approximately 1 cm^3. These fragments were freeze-dried to remove any moisture without altering the pore structure (Koliji et. al, 2010). For this purpose, the samples were first introduced in liquid nitrogen at – 196℃, then left in a freeze-dryer for 24 hours to allow vacuum drying of the frozen samples via sublimation (Delage et. al 1996). The dry samples were placed in a penetrometer, which was then positioned in the low-pressure chamber. The system was initially evacuated under vacuum, and the samples were subsequently filled with mercury (a non-wetting fluid) as the pressure gradually increased to atmospheric levels. The intrusion pressure was then raised to approximately 206 kPa using compressed air. After depressurization to ambient conditions, the samples were transferred to high-pressure chamber, where mercury intrusion continued by increasing the pressure up to 414 MPa. The detected entrance pore diameters range between 364 μm and 0.003 μm.

2.3.3 Unconfined compressive strength test

UCS tests were conducted, according to the ASTM D2166 standards, on stabilized cylindrical samples with 72 mm height and 36 mm diameter after 0, 7, 28 and 60 days of curing. The UCS tests were conducted at an axial displacement rate of 0.0667 mm/min. Each test continued until either failure surfaces were clearly visible or an axial strain of 20% was reached. To ensure consistency and reproducibility, three identical samples with the same mix proportion and curing time were tested each time, and the average results, along with their standard deviation, were reported.

3 RESULTS AND DISCUSSION

3.1 Proctor compaction properties

The compaction curves of the MLD and the MLD blended with 5% GGBS and distilled water (reference mix), shown in Figure 2, show that the MDD decreases, and the OMC increases with the addition of 5% GGBS to the soil. The addition of GGBS modifies the soil matrix by filling voids with finer particles, which can hinder the rearrangement of larger grains during compaction and limit the achievement of a denser structure. In addition, the increased surface area from the fine GGBS particles, combined with their pozzolanic nature, demands more water for particle coating and hydration reactions, leading to an increase in the OMC. This decrease in the MDD and increase in the OMC is also observed for other soils when mixed with fine materials such as lime or fly ash (Okeke et. al 2019, Güneyli 2010, Turan et. al 2022, De Bel et. al 2013).

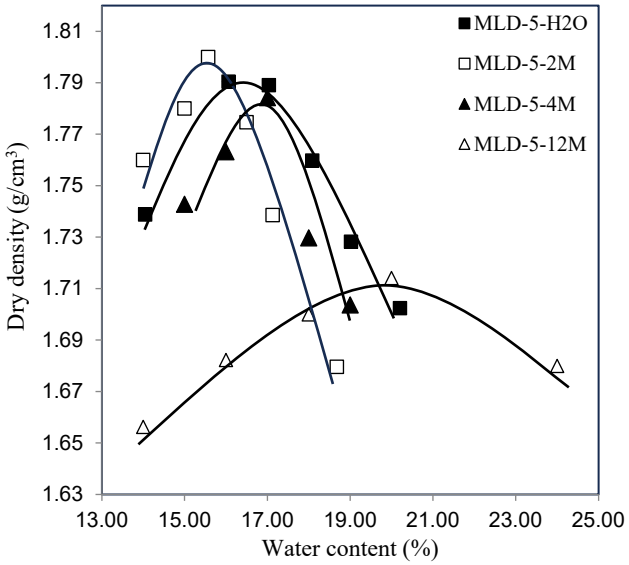

Figure 3: Proctor compaction curves

The compaction curves of the mixtures stabilized with 5% GGBS and NaOH with different concentrations, presented in Figure 3, show different effects of NaOH activation on the soil's compaction behavior. Compared to MLD-5-H2O, which reaches a MDD of 1.79 g/cm³ at an OMC of about 16.5%, the inclusion of NaOH leads to a variation in the MDD and a shift of the OMC. The direction of this shift varies with the concentration of NaOH. The MLD-5-2M mixture shows a slight increase in MDD and a shift of the OMC toward lower water content. In contrast, the MLD-5-4M and MLD-5-12M

mixtures exhibit a progressive reduction in MDD and a shift of the OMC toward higher water contents, with MLD-5-12M reaching the lowest dry density (1.70 g/cm³) and the highest OMC (21%).

This observed reduction in MDD and increase in OMC with increasing NaOH concentration can be explained by the changes in the physicochemical environment of the soil-water system introduced by alkali activation. In particular, the interaction of water molecules with the Na^+ and OH^- ions in the alkaline solution plays a crucial role. In NaOH solutions, a significant portion of the water becomes bound in the form of hydration shells surrounding the dissolved ions (Na^+ and OH^-) (Ma et. al 2024). Each Na^+ ion typically attracts several water molecules, forming a stable hydration sphere due to electrostatic interactions. Similarly, OH^- ions also engage water molecules through hydrogen bonding. This results in a reduction of free water, which is the fraction available to lubricate soil particles and facilitate particle rearrangement during compaction. As the NaOH concentration increases, the number of hydrated ions also increases, thereby increasing the fraction of bound water and reducing the effective free water content needed for optimal compaction. Consequently, higher water content is required to compensate for the bound water and achieve sufficient workability during compaction, leading to the observed shift of the OMC toward higher values. At the same time, higher NaOH concentrations significantly increase the viscosity of the fluid, which has direct impact on the compaction behavior of the mixture. High viscosity impairs the ability of soil particles to rearrange and densify under compaction, as the thickened fluid phase resists particle movement and hinders the expulsion of entrapped air. This results in a less efficient packing of the solid matrix, leading to lower MDD and greater heterogeneity within the compacted soil.

Inversely, the 2M NaOH mixture exhibited a slight shift in OMC toward lower values compared to the non-activated GGBS mixture. This suggests that at low concentrations, the amount of Na^+ and OH^- ions is low enough that the extent of hydration shell formation remains limited, preserving a larger fraction of free water for lubrication and particle rearrangement during compaction. Moreover, the mild flocculation of particles induced by low ionic strength may improve particle gradation and packing efficiency, resulting in a denser compacted structure (Abdullah et. al 2020).

3.2 Pore size distribution

The MIP test results presented in Figure 4 reveal the influence of the activator concentration on the pore size distribution of the stabilized soil at day 0 (after compaction). The reference mix (MLD-5-H2O) shows a single family of pores with a peak centered around 1 μm, indicating a predominance of larger capillary pores. Smaller micropores (< 10 nm) are also observed, but only to a limited extent. On the other hand, in the presence of alkali solutions, all the samples show the emergence of a new family of larger pores around 9 μm, regardless of the concentration. The addition of NaOH has limited influence on the micropores. The emergence of this new family of large pores upon the addition of NaOH, even prior to any curing or formation of reaction products, indicates that the alkaline environment itself alters the initial microstructure of the soil-GGBS matrix. This behavior can be attributed to structural dispersion caused by changes in the surface charge at the edges of clay particles (Chavali et al., 2017). The resulting acid-base attack occurs rapidly, increasing repulsive forces and leading to macropore generation (Barakat et al., 2024; Shao et al. 2024). This confirms that the presence of NaOH induces structural rearrangement at the particle level, even before the development of alkali-activated gels such as C-A-S-H. Notably, the 12M NaOH mixture shows a reduction in the peak intensity associated with smaller pores (around 1 μm) and a pronounced increase in the peak at larger pore sizes (around 9 μm), indicating a coarser and more open initial pore network.

3.3 Unconfined compressive strength

UCS tests were conducted on stabilized samples with varying concentrations of the NaOH solution (2M, 4M, and 12M) after 0, 7, 28 and 60 days of curing. The results of the UCS tests are presented in Figure 5, with error bars indicating the standard deviation of the three tests performed. The results demonstrate good reproducibility of the experimental data. Overall, independent of the activator's concentration, the UCS of the alkali-activated GGBS-stabilized soil consistently increased over time due to the ongoing chemical reactions and

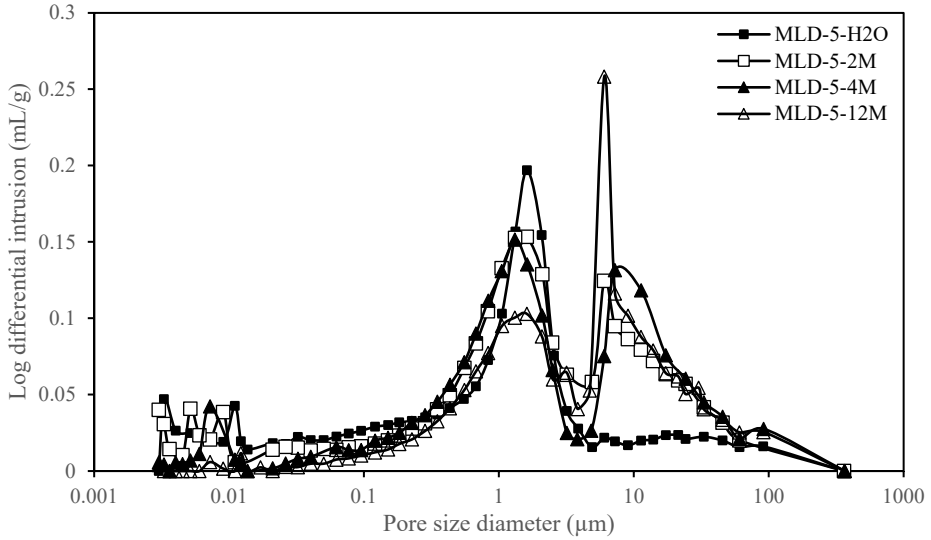

Figure 4: Pore size distribution of samples with different concentrations of NaOH at 0 days of curing.

the gradual formation of stronger bonds within the soil matrix. Moreover, regardless of the activator concentration, the soil stabilized with alkali-activated GGBS showed a significant increase in the UCS compared to the GGBS stabilized soil, even after just 7 days of curing. This strength increase can be attributed to the high pH of the NaOH solution, which enhances the dissolution of silica (SiO_2), alumina (Al_2O_3), and calcium (CaO) present in the GGBS (Sahoo & Prasad Singh 2022). This dissolution releases silicate, aluminate, and calcium ions into the solution, promoting the formation of cementitious compounds such as (N,C)-A-S-H gels, which are primarily responsible for strength development in the stabilized soil. In contrast, in water (as in the case of GGBS-stabilized soil), the near-neutral pH is insufficient to significantly dissolve the GGBS components, resulting in limited reaction and strength gain.

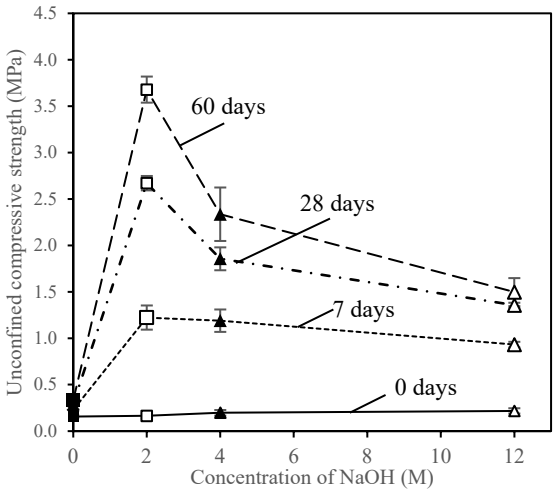

Figure 5: UCS results at 0, 7, 28 and 60 days.

On the other hand, samples with a NaOH concentration of 2M reached the highest UCS compared to samples with other concentrations, across all curing times, reaching a peak of approximately 3.7 MPa at 60 days. Higher concentrations of 4M and 12M result in reduced strength gains, particularly at longer curing times, with UCS values of around 2.3 MPa and 1.5 MPa at 60 days, respectively.

All samples were compacted at the same MDD and OMC, determined from the MLD-5-H2O reference mixture. However, applying a uniform compaction point across all formulations does not account for the distinct water demands introduced by varying alkali concentrations. At higher NaOH concentrations, a significant portion of the mixing water becomes chemically bound in hydration shells around Na^+ and OH^- ions or is consumed in the early formation of reaction products. This reduces the proportion of free water available for workability, reaction transport, and continued hydration. As a result, although the total moisture content remained constant across all mixtures, the effective moisture content (the water available to sustain reaction kinetics and internal curing) was significantly lower in the 12M mixture. This limited the extent of GGBS activation, which in turn hindered the development of a dense and cohesive binder phase and ultimately reduced strength. Furthermore, the low availability of free water negatively affects compaction by increasing the mixture stiffness, reducing workability and limiting the uniformity of the compacted matrix affecting negatively strength.

In contrast, the 2M mixture maintained a better balance between activation potential and available water, supporting continuous gel formation and strength development over time, which led to superior UCS performance. These findings highlight that, in alkali-activated systems, strength development is not only governed by chemical composition but is also highly sensitive to the internal water dynamics. Using the same compaction parameters for all mixtures can disadvantage high-molarity systems due to their increased chemical water demand and reduced free water availability.

3.3 Correlation between compaction and strength

The test results indicated a clear relationship between the compaction characteristics and the UCS of the alkali-activated mixtures examined in this study. The Proctor test results showed that increasing NaOH molarity led to a reduction in MDD and a shift in OMC to higher values, particularly in the 4M and 12M mixtures. This trend reflects the increasing proportion of bound water due to ion hydration and early gel formation, which reduces the availability of free water during compaction and limits particle rearrangement. These same mechanisms influence strength development. Although higher NaOH concentrations increase chemical activation potential, the reduced effective moisture content impairs the formation of a well-connected and dense microstructure, which is essential for strength gain. In contrast, the 2M mixture achieves a better balance, maintaining relatively high compactability and sufficient activation, leading to the highest UCS over time. These results highlight that optimal strength in alkali-activated soils is not achieved through maximum chemical activation alone, but through a balance between compaction efficiency, water availability, and reaction kinetics.

4 CONCLUSIONS

This study investigated the influence of NaOH concentration on the compaction behavior and UCS development of a clayey silt stabilized with 5% alkali-activated GGBS.

At low concentrations, the alkali activation is sufficient to initiate beneficial interactions between the soil and GGBS without significantly binding the mixing water or forming obstructive early-stage reaction products, leading to better compaction and increased strength. However, at higher molarities (4M and 12M), the dominance of bound water and early-stage reaction products becomes detrimental to compaction efficiency as well as the progression of the chemical reactions responsible for strength development. Moreover, the alkaline environment created by the addition of the activator, regardless of its concentration, creates dispersion of particles within the mixture, as evidenced by the appearance of a larger class of pores observed even at 0 days of curing, before the formation of any reaction products.

For future research, it would be interesting to consider optimizing the compaction parameters (i.e. moisture content) for each NaOH concentration individually in order to get optimal strength without the excessive use of the activator. In addition, thermogravimetric analysis (TGA) could be used to quantify the free and bound water available in the mixture, providing experimental validation of the proposed hypothesis. Furthermore, developing a predictive model based on these parameters could offer valuable insights into strength development and support more efficient mix design.

5 REFERENCES

Abdullah, H.H., Shahin, M.A., Walske, M.L. and Karrech, A. (2020) Systematic approach to assessing the applicability of fly-ash-based geopolymer for clay stabilization, *Canadian Geotechnical Journal*, 57(9), pp. 1356–1368.

Alahmari, T.S., Abdalla, T.A. and Rihan, M.A.M., 2023. Review of recent developments regarding the durability performance of eco-friendly geopolymer concrete. *Buildings*, 13(12), p.3033.

Al-Rkaby, A.H.J., 2019. Evaluating shear strength of sand-GGBFS based geopolymer composite material. *Acta Polytechnica*, 59, pp.305–311.

Alsalman, A., Assi, L.N., Kareem, R.S., Carter, K. and Ziehl, P., 2021. Energy and CO_2 emission assessments of alkali-activated concrete and Ordinary Portland Cement concrete: A comparative analysis of different grades of concrete. *Cleaner Environmental Systems*, 3, January.

ASTM International, 2000. *ASTM D2487-00: Standard classification of soils for engineering purposes (Unified Soil Classification System)*. West Conshohocken, PA: ASTM International.

ASTM International, 2017. *ASTM D4318-17e1: Standard test methods for liquid limit, plastic limit, and plasticity index of soils*. West Conshohocken, PA: ASTM International.

ASTM International, 2021. *ASTM D698-12(2021): Standard test methods for laboratory compaction characteristics of soil using standard effort (12,400 ft-lbf/ft³ (600 kN-m/m³))*. West Conshohocken, PA: ASTM International.

ASTM International, 2013. *ASTM D2166-13: Standard test method for unconfined compressive strength of cohesive soil*. West Conshohocken, PA: ASTM International.

Barakat, Y., Mokni, N., Cui, Y-J. and Bernier, F., 2024. Effects of salinity and alkalinity on the volumetric deformation of the Opalinus Clay from the Lower Sandy Facies (LSF) of Mont Terri site. *Rock Mechanics and Rock Engineering*, 57, pp.9251–9273.

Chami, D., Schmitz, V., Gerard, P. & Cuccurullo, A. 2024. *Mechanical and durability properties of GGBS-based geopolymer stabilized earth*. In: *Proceedings of the 2nd RILEM International Conference on Earthen Construction (ICEC2024)*, Edinburgh, United Kingdom.

Chavali, R.V.P., Vindula, S.K., Reddy, H.P., Babu, A. and Pillai, R., 2017. Swelling behavior of kaolinitic clays contaminated with alkali solutions: a micro-level study. *Applied Clay Science*, 135, pp.575–582.

Coudert, E., Deneele, D., Russo, G., Vitale, E. & Tarantino, A. 2021. *Microstructural evolution and mechanical behaviour of alkali activated fly ash binder treated clay*. *Construction and Building Materials*, 285, 122917.

Cristelo, N., Glendinning, S., Miranda, T., Oliveira, D. and Silva, R., 2012. Soil stabilization using alkaline activation of fly ash for self-compacting rammed earth construction. *Construction and Building Materials*, 36, pp.727–735.

Davidovits, J., 2002. 30 years of successes and failures in geopolymer applications: market trends and potential breakthroughs. Presented at the Geopolymer 2002 Conference, 28–29 October 2002.

De Bel, R., Gomes Correia, A., Duvigneaud, P.H., François, B., Herrier, G. and Verbrugge, J.C., 2013. Evolution mécanique et physico-chimique à long terme d'un sol limoneux traité à la chaux. In: *Colloque Terdouest*, Paris, France.

Delage, P., Audiguier, M., Cui, Y.-J. and Howat, M.D., 1996. *Microstructure of a compacted silt*. Canadian Geotechnical Journal, 33(1), pp.150–158.

Gerard, P., Mahdad, M., McCormack, A.R. & François, B., 2015. A unified failure criterion for unstabilized rammed earth materials upon varying relative humidity conditions. *Construction and Building Materials*, 95, pp.437–447.

Ghadir, P. and Ranjbar, N., 2018. Clayey soil stabilization using geopolymer and Portland cement. *Construction and Building Materials*, 188, pp.361–371.

Güneyli, H., 2010. Influence of Afşin-Elbistan highly limy fly ash on engineering behavior of a cohesive soil. Scientific Research and Essays, 5(11), pp.1307–1316.

Koliji, A., Vulliet, L. and Laloui, L., 2010. *Structural characterization of unsaturated aggregated soil*. Canadian Geotechnical Journal, 47(3), pp.297–311

Ma, R., Baradwaj, N., Nomura, K., Krishnamoorthy, A., Kalia, R.K., Nakano, A. and Vashishta, P. (2024) 'Alkali hydroxide (LiOH, NaOH, KOH) in water: Structural and vibrational properties, including neutron scattering results', *The Journal of Chemical Physics*, 160(13), 134309.

Myers, R.J., Bernal, S.A., Nicolas, R.S. and Provis, J.L., 2013. Generalized structural description of calcium sodium aluminosilicate hydrate gels: the cross-linked substituted tobermorite model. *Langmuir*, 29.

Okeke, C.A.U., Johnson, A.O., Ogbuagu, F.U. and Akinmusuru, J.O., 2019. Effects of continuous leaching on engineering properties of lime-stabilized lateritic soils. In: 1st International Conference on Sustainable Infrastructural Development. IOP Conference Series: Materials Science and Engineering, 640, 012084.

Onuki, A., Araki, T. and Okamoto, R., 2011. Solvation effects in phase transitions in soft matter. *Journal of Physics: Condensed Matter*, 23(28), p.284113.

Sahoo, S. and Prasad Singh, S., 2022. Strength and durability properties of expansive soil treated with geopolymer and conventional stabilizers. *Construction and Building Materials*, 328(January), p.127078.

Shao, J., Sun, D., Peng, F. and Zeng, Z., 2024. Effect of alkaline solution on hydraulic and mechanical properties of MX80 granular bentonite. *Annals of Nuclear Energy*, 209, p.110822.

Turan, C., Javadi, A.A. and Vinai, R., 2022. *Effects of Class C and Class F fly ash on mechanical and microstructural behavior of clay soil—A comparative study*. Materials, 15(5), p.1845.